

# Lawrence Berkeley National Laboratory

## LBL Publications

### Title

A vacuum ultraviolet photoionization study on the thermal decomposition of ammonium perchlorate

### Permalink

<https://escholarship.org/uc/item/9mn532jk>

### Authors

Góbi, Sándor  
Zhao, Long  
Xu, Bo  
et al.

### Publication Date

2018

### DOI

10.1016/j.cplett.2017.11.026

Peer reviewed

# **A Vacuum Ultraviolet Photoionization Study on the Thermal Decomposition of Ammonium Perchlorate**

Sándor Góbi<sup>1</sup>, Long Zhao<sup>1</sup>, Bo Xu<sup>2</sup>, [Utuq Ablikim](#)<sup>2</sup>, Musahid Ahmed<sup>2</sup>, Ralf I. Kaiser<sup>1,\*</sup>

<sup>1</sup> Department of Chemistry, University of Hawai'i at Mānoa, Honolulu, HI 96822, USA

W.M. Keck Laboratory in Astrochemistry, University of Hawai'i at Mānoa, Honolulu, HI 96822, USA

<sup>2</sup> Chemical Sciences Division, Lawrence Berkeley National Laboratory, Berkeley, California 94720, USA.

[ralfk@hawaii.edu](mailto:ralfk@hawaii.edu)

## ABSTRACT

Pyrolysis products of ammonium perchlorate ( $\text{NH}_4\text{ClO}_4$ ) ~~samples~~ at 483 K were monitored on line and *in situ* via single photon photoionization reflectron time-of-flight spectrometry (PI-ReTOF-MS) in the photoionization range of 9.00–17.50 eV. The photoionization ~~energy~~ efficiency curves (PIE) of the subliming product molecules were collected and allowed for ~~the~~ detection of three class of products ~~covering~~ containing chlorine, nitrogen, and oxygen ~~containing compound~~ including atoms and free radicals. ~~These results suggest new insight into~~ is ~~work also aims to shed light on the~~ possible low-temperature decomposition pathways of  $\text{NH}_4\text{ClO}_4$ .

## 1. INTRODUCTION

~~During the last 50 years, the~~The degradation of ~~the~~ ammonium perchlorate ( $\text{NH}_4\text{ClO}_4$ ) – widely exploited as a solid rocket propellant – has been extensively studied both experimentally and computationally for half a century. ~~However~~Yet, the exact decomposition mechanisms and distinction between *primary* and *higher order products* have remained elusive to date.<sup>1</sup> Previous investigations ~~have converged~~suggest that ammonium perchlorate ~~holds~~has two distinct decomposition pathways at “low” (below 510 K) and “high” temperatures (above 620 K); ~~The~~ first step in the thermal decomposition has been proposed to be initiated by a proton transfer from the ammonium moiety ( $\text{NH}_4^+$ ) to the perchlorate anion ( $\text{ClO}_4^-$ ) resulting in the formation of ammonia ( $\text{NH}_3$ ) and perchloric acid ( $\text{HClO}_4$ , ~~R1~~); ~~These~~ primary decomposition products can take part in multiple consecutive reactions.<sup>1-6</sup>



Bircumshaw and Newman (1954) pioneered the experimental investigations examining the thermolysis of ammonium perchlorate ( $\text{NH}_4\text{ClO}_4$ ) *in vacuo* in the temperature ranges of 493–553 and 653–723 K (Table 1).<sup>7</sup> The authors concluded that at low temperatures, only 30% of the reactant decays; the solid residue was found to be porous suggesting that the decomposition takes place throughout the material. Furthermore, a phase transition of ammonium perchlorate from orthorhombic to cubic was observed at 513 K. Finally, this work detected multiple gaseous decomposition products at low temperatures: molecular chlorine ( $\text{Cl}_2$ ), nitrous oxide ( $\text{N}_2\text{O}$ ), dinitrogen tetroxide ( $\text{N}_2\text{O}_4$ ), molecular oxygen ( $\text{O}_2$ ), nitrogen ( $\text{N}_2$ ), water ( $\text{H}_2\text{O}$ ), hydrogen chloride ( $\text{HCl}$ ), chlorine dioxide ( $\text{ClO}_2$ ), and perchloric acid ( $\text{HClO}_4$ ).

The first mass ~~spectroscopic~~spectrometric (MS) detection of the decomposition products was ~~achieved~~performed by Heath and Majer.<sup>8</sup> This study revealed that the decomposition takes place in the solid phase with the predominant fragmentation leading to gas-phase ammonia ( $\text{NH}_3$ ) and perchloric acid ( $\text{HClO}_4$ ); this finding was corroborated by Inami et al.<sup>2</sup> A subsequent MS study concluded that the thermal decomposition of ammonium perchlorate yielded principally water ( $\text{H}_2\text{O}$ ), nitrous oxide ( $\text{N}_2\text{O}$ ), dichlorine ( $\text{Cl}_2$ ), and oxygen ( $\text{O}_2$ ) along with hydrogen chloride ( $\text{HCl}$ ) and molecular nitrogen ( $\text{N}_2$ ).<sup>9</sup> Gas chromatography (GC) was also applied to detect the thermolysis products as oxygen ( $\text{O}_2$ ), nitrogen ( $\text{N}_2$ ), nitrous oxide ( $\text{N}_2\text{O}$ ), dichlorine ( $\text{Cl}_2$ ), chlorine dioxide ( $\text{ClO}_2$ ), nitric acid ( $\text{HNO}_3$ ), hydrogen chloride ( $\text{HCl}$ ), and nitrogen monoxide

(NO).<sup>10</sup> Mechanistical studies proposed that the low-temperature decay represents an autocatalytic process starting with the decomposition of ammonium perchlorate ( $\text{NH}_4\text{ClO}_4$ ) to adsorbed ammonia ( $\text{NH}_3$ ) and perchloric acid ( $\text{HClO}_4$ ) followed by autoprotection transforming the primary perchloric acid product into water ( $\text{H}_2\text{O}$ ) plus the chlorine trioxide cation ( $\text{ClO}_3^+$ ); the latter was speculated to oxidize ammonia to higher order products such as nitrogen oxides as observed.<sup>11,12</sup>

Further, an attenuated total reflection (ATR) infrared study confirmed the phase transition at 513 K; however, this study could not detect any new species formed in the solid or in gas phase.<sup>13</sup> The time-of-flight (TOF) mass spectrometry (MS) coupled with electron impact (EI) was first utilized by Boldyrev et al. detecting not only the primary decomposition products ammonia ( $\text{NH}_3$ ) and perchloric acid ( $\text{HClO}_4$ ), but also chlorine trioxide ( $\text{ClO}_3$ ), chlorine dioxide ( $\text{ClO}_2$ ), chlorine monoxide ( $\text{ClO}$ ), chlorine atom ( $\text{Cl}$ ), and amidogen ( $\text{NH}_2$ ).<sup>14</sup> Hackman et al. exploited TOF-MS and observed the nitrosyl hydride ( $\text{HNO}$ ) for the first time.<sup>15</sup> Besides, hydrides of nitrogen other than ammonia ( $\text{NH}_3$ ) such as the ammonium radical ( $\text{NH}_4$ ), amidogen ( $\text{NH}_2$ ), and imidogen ( $\text{NH}$ ) might also play a role in the decomposition mechanisms. Perchloric acid ( $\text{HClO}_4$ ), atomic chlorine ( $\text{Cl}$ ), and simple chlorine oxides like chlorine oxide ( $\text{ClO}$ ), chlorine dioxide ( $\text{ClO}_2$ ), and chlorine trioxide ( $\text{ClO}_3$ ) radicals were found, too. However, no evidence was presented for dichlorine ( $\text{Cl}_2$ ), hypochloric acid ( $\text{HOCl}$ ), chlorous acid ( $\text{HClO}_2$ ), chloric acid ( $\text{HClO}_3$ ), chlorine tetroxide ( $\text{ClO}_4$ ), molecular nitrogen ( $\text{N}_2$ ), nitrous oxide ( $\text{N}_2\text{O}$ ), and nitrogen dioxide ( $\text{NO}_2$ ) as detected in prior studies. Here, the authors proposed the decay of perchloric acid ( $\text{HClO}_4$ ) into chlorine trioxide ( $\text{ClO}_3$ ) and hydroxyl radicals ( $\text{OH}$ ) as opposed to an autoprotection process. Subsequently, Brill and Goetz utilized Raman spectroscopy to monitor the phase change in ammonium perchlorate between 300 and 625 K.<sup>16</sup> Galwey and Mohamed speculated on nitryl perchlorate ( $\text{NO}_2\text{ClO}_4$ ) as a reaction intermediate based on its high thermal instability and the observation of oxidized nitrogenous species like nitrogen monoxide cation ( $\text{NO}^+$ ).<sup>17</sup>

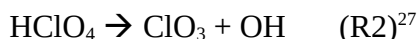
The use of differential scanning calorimetry (DSC), high-pressure liquid chromatography (HPLC), and gas chromatography (GC) revealed the presence of oxygen ( $\text{O}_2$ ), nitrogen ( $\text{N}_2$ ), dichlorine ( $\text{Cl}_2$ ), chloride ( $\text{Cl}^-$ ), chlorate ( $\text{ClO}_3^-$ ), nitrous oxide ( $\text{N}_2\text{O}$ ), and the ammonium cation ( $\text{NH}_4^+$ ).<sup>18</sup> Low-temperature decomposition of ammonium perchlorate ( $\text{NH}_4\text{ClO}_4$ ) and its partly

and/or completely deuterated isotopologue ( $\text{NH}_{4-x}\text{D}_x\text{ClO}_4$ ) was examined by Majda et al. via DSC, SEM, thermogravimetric analysis (TGA), and quadrupole MS (QMS) techniques.<sup>19,20</sup> These studies ~~exposed~~ showed that the **decay rate depends on the degree of deuteration**; furthermore, the volume fraction of the pores of the deuterated sample appears to be lower compared to the non-labeled counterpart. The authors concluded that the effects can be best rationalized as caused by a proton transfer at the intersections of dislocations in the bulk of the crystals. Nitrous oxide ( $\text{N}_2\text{O}$ ) and nitrogen monoxide ( $\text{NO}$ ) were detected via MS as decomposition products of the low-temperature and high-temperature decomposition, respectively.

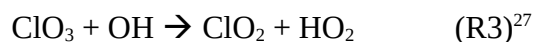
Thereafter, a TGA/DSC-MS/FT-IR analysis showed that the formation of nitrous oxide ( $\text{N}_2\text{O}$ ) and nitrogen dioxide ( $\text{NO}_2$ ) is strongly temperature dependent.<sup>21</sup> Three distinct decomposition stages were proposed: an autocatalytic pathway, a low-temperature diffusion, and a high-temperature stable-phase reaction. The degradation occurs inside the pores of the sample beneath the surface, where the primary products ammonia ( $\text{NH}_3$ ) and perchloric acid ( $\text{HClO}_4$ ) are adsorbed. The latter ~~one~~ adsorbs more rapidly thus the concentration of ammonia in the gas phase was found to be higher. As perchloric acid decomposes into other chlorine oxides like chlorine dioxide ( $\text{ClO}_2$ ), these oxides were suggested to facilitate the gas-phase oxidation of ammonia ( $\text{NH}_3$ ).<sup>1</sup> At high temperatures, the products formed inside the sample can take part in higher order subsequent reactions both at the surface and in the gas phase. Recent TGA-FT-IR/EI-MS studies detected nitrous oxide ( $\text{N}_2\text{O}$ ) as the primary product of the low-temperature degradation of ammonium perchlorate ( $\text{NH}_4\text{ClO}_4$ ) followed by hydrogen chloride ( $\text{HCl}$ ), nitrogen dioxide ( $\text{NO}_2$ ), and nitric acid ( $\text{HNO}_3$ ).<sup>22,23</sup> Water ( $\text{H}_2\text{O}$ ), dichlorine ( $\text{Cl}_2$ ), and oxygen ( $\text{O}_2$ ) were observed via the electron ionization mass spectrometry. Interestingly, nitrogen monoxide ( $\text{NO}$ ) could not be identified. The effect of grain size was also probed.<sup>23</sup> Kinetic studies and the effect of pressure on the degradation mechanisms were investigated exploiting TGA and DSC methods and are summarized in Table S1 in the Supplementary Material.

Extensive theoretical studies have also been conducted.<sup>24</sup> The computational efforts by Lin et al. proposed the mechanism and determined rate constants of reactions that occur during the thermolysis of ammonium perchlorate.<sup>25,26</sup> The calculations agree with the experimental results

and consider R1 as the first reaction that takes place during the pyrolysis, followed by the unimolecular decomposition of perchloric acid into chlorine trioxide and hydroxyl radical:



which is succeeded by the reaction of the product molecules into chlorine dioxide ( $\text{ClO}_2$ ) and hydroperoxyl radical ( $\text{HO}_2$ ):



The unimolecular decomposition of the chlorine oxides ( $\text{ClO}_x$ ) by atomic oxygen loss might also be an important pathway.<sup>28,29</sup> The forming oxygen atoms ( $\text{O}$ )<sup>30</sup> and chlorine oxides ( $\text{ClO}_x$ ,  $x = 1-3$ )<sup>31</sup> may for instance take part in the oxidation of ammonia ( $\text{NH}_3$ ), therefore accounting for the formation of various nitrogen oxides ( $\text{N}_x\text{O}_y$ ). The reaction of oxidants with the ammonia decomposition product amidogen ( $\text{NH}_2$ ) was also investigated by theoretical methods.<sup>32,33</sup>

However, despite extensive investigations, no coherent picture has emerged to date on the reaction pathways and products during the thermolysis of ammonium perchlorate within a single experimental setup. Strong discrepancies between the experimental and theoretical results are evident.<sup>1,25,34</sup> The present work aims to present a comprehensive, unbiased picture on *all products exploiting a single, versatile experimental technique* that may be important during the thermolysis of ammonium perchlorate by detecting *all* degradation products for the first time under controlled conditions on line and *in situ* via state-of-the-art single vacuum ultraviolet (VUV) photoionization coupled with reflectron time-of-flight mass spectrometry (PI-ReTOF-MS). Compared to traditional mass spectrometry exploiting EI and off line GC-MS and HPLC analysis, this technique has unique advantages. The EI results not only in the ionization of the parent molecule, but also in its extensive fragmentation; furthermore, the structural isomers cannot be easily distinguished in most of the cases as only their fragmentation pattern may give structural information, which can be dubious. These can be easily avoided by using the PI-ReTOF-MS technique since the ionization energy (*IE*) can be chosen thus the fragmentation does not take place.<sup>35</sup> Moreover, the structural isomers can also easily be separated based on their distinct *IEs and PIE curves*.<sup>36</sup> The on line and *in situ* detection of the product molecules prevents the disadvantage of HPLC and GC-MS, i.e. undesirable side-reactions that can occur between the

experiment and the measurement,<sup>37</sup> for instance at high-temperatures in the case of GC-MS<sup>38,39</sup> or in the solution phase when using the HPLC technique.

## 2. EXPERIMENTAL DETAILS

The experiments were conducted at the Advanced Light Source (ALS) at the Chemical Dynamics Beamline (9.0.2.). The main apparatus consists of a high vacuum chamber equipped with a reflectron time of flight mass spectrometer (Re-TOF-MS) and a bankable sample reservoir mounted below the ion optics of a spectrometer in the detection chamber.<sup>40</sup> Ammonium perchlorate (50 mg, 99.5%, Sigma-Aldrich) was placed in this aluminum container and heated by a 50  $\Omega$  resistance to  $483 \pm 2$  K as monitored by a Type-K thermocouple (Figure 1). The gaseous products were ~~then~~ photoionized between the repeller and extractor of the Re-TOF-MS by exploiting quasi-continuous tunable vacuum ultraviolet (VUV) synchrotron light filtered by argon or helium, and detected with ~~a~~ microchannel plates ~~(MCP)~~. The photoionization efficiency (PIE) curves, which report the intensity of a single mass-to-charge ratio ( $m/z$ ) versus the photon energy, were extracted from these mass spectra recorded over a range from 9.00 eV to 17.50 eV in steps of 0.05 eV by integrating the signal collected at a specific  $m/z$  over the range of photon energies and normalized to the incident photon flux.<sup>41,42</sup> This range covers the *IEs* of all the species generated in the pyrolysis process. The PIE curves are exploited to unambiguously identify the decomposition species including radicals and closed-shell products.<sup>43-48</sup> PIE curve fittings were performed to identify the species detected and compared with reference PIE curves.<sup>49</sup>

## 3. RESULTS

The experimental data obtained by the PI-ReTOF-MS apparatus upon the pyrolysis of ammonium perchlorate ( $\text{NH}_4\text{ClO}_4$ ) are visualized in Figure 2. The most intense peaks at the lowest photon energy displayed (12.0 eV, Figure 2a) ~~can be found at the  $m/z$  values of 70 and 72~~ are  $m/z$  70 and 72, along with minor signals at  $m/z = 17, 30, 32, 46, 51, 52, 53, 54, 62, 63, 67, 69,$  and 74, respectively. With increasing VUV photon energies (14.0 eV, Figure 2b) the peak at  $m/z = 18$  becomes predominant. Besides the already established signals detected at lower energies, new mass-to-charge ratios emerge at  $m/z = 16, 35, 36, 37, 38, 44, 83, 85, 100,$  and 102, respectively. At a photoionization energy of 16.0 eV (Figure 2c), the most important peaks are at  $m/z = 18, 32,$

44, 70, and 72; however, signal at mass-to-charge ratios of 16, 28, 35, 36, 37, 46, 74, and 100 can also be detected. Figure 2d shows the spectrum obtained at the VUV photon energy of 17.5 eV, which correlates well with the results obtained at 16.0 eV; this spectrum differs only in the relative signal strengths. The signal observed at distinct photoionization energies along with their assignments are summarized in Table 2; the determined PIE curves are discussed in Section 4.1.

## 4. DISCUSSION

### 4.1. Interpretation of the PIE data.

The PIE curves derived from the PI-ReTOF-MS spectra are shown in Figure 3. The PIE curve of the perchloric acid isotopologues ( $^{35}\text{HClO}_4$  and  $^{37}\text{HClO}_4$ ,  $m/z = 100$  and  $102$ ) are plotted in Figures 3a and 3b. Although the PIE curve cannot be compared with literature PIE curve as it has not been recorded to date, the ionization [energy](#) ( $IE = 12.37$  eV) agrees well with the literature data of the adiabatic ionization energy of  $12.37$  eV ( $IE_{\text{ad}}$ , Table 2). Tables S2 and S3 in Supplementary Information summarize the references used for the  $IE_{\text{ad}}$  and PIE data. The same holds true for chlorine trioxide isotopologues ( $^{35}\text{ClO}_3$  and  $^{37}\text{ClO}_3$ ,  $m/z = 83$  and  $85$ , Figures 3c and 3d); the  $IE$  values ( $11.47$  eV) agree well with the  $IE_{\text{ad}}$  of  $11.4 \pm 0.1$  eV as determined previously. Furthermore, the possibility that perchloric acid ( $\text{HClO}_4$ ) may photofragment into chlorine trioxide at higher photon energies cannot be ruled out completely. Molecular chlorine ( $\text{Cl}_2$ ) is revealed at  $m/z = 70, 72,$  and  $74$  (Figures 3e–3g); the experimentally determined onset of the ion signals of  $11.47$  eV is close to their  $IE_{\text{ad}}$  values of  $11.48 \pm 0.01$  eV; and the PIE curves show similarity with previous experimental results.

The  $IE_{\text{ad}}$  value of chlorine dioxide isotopologues ( $^{35}\text{ClO}_2$  and  $^{37}\text{ClO}_2$ ,  $m/z = 67$  and  $69$ ) of  $10.33 \pm 0.02$  eV correlates well with our onset of ion signal of  $10.37$  eV (Figures 3h and 3i). Their PIE curves slightly differ from the literature data, which can be explained by fragmentation of perchloric acid ( $\text{HClO}_4$ ) or chlorine trioxide ( $\text{ClO}_3$ ). The  $IE_{\text{ad}}$  of nitric acid ( $\text{HNO}_3$ ,  $m/z = 63$ ) of  $11.95 \pm 0.01$  eV nicely corresponds to the onset of ion signal at  $11.97$  eV (Figure 3j); the experimental PIE curve is close to literature data. In contrast, although nitrogen trioxide ( $\text{NO}_3$ ) is expected to be the main product detected at  $m/z = 62$  with an adiabatic ionization energy of  $12.57 \pm 0.02$  eV (Figure 3k), both nitramide ( $\text{NH}_2\text{NO}_2$ ) and hyponitrous acid ( $\text{HON}=\text{NOH}$ ) may contribute to the overall signal, which holds on onset of  $11.02$  eV. The PIE curve of nitrogen trioxide ( $\text{NO}_3$ ) was determined previously showing similarities with the one determined by the

current study at VUV photon energies above its the adiabatic ionization energy. It is worth noting that according to previous studies, the photofragmentation of nitric acid ( $\text{HNO}_3$ ) does not yield nitrogen trioxide fragments ( $\text{NO}_3$ ).

The onset of ionization of 11.07 eV obtained for the hypochlorous acid isotopologues ( $^{35}\text{HOCl}$  and  $^{37}\text{HOCl}$ ,  $m/z = 52$  and  $54$ , Figures 3l and 3n) agree with their adiabatic ionization energy of  $11.12 \pm 0.01$  eV ~~as well~~. The literature PIE curve is also comparable to our experimentally recorded data ~~as well~~. Our PIE curves for chlorine monoxide ( $^{35}\text{ClO}$  and  $^{37}\text{ClO}$ ,  $m/z = 51$  and  $53$ ) have some discrepancies at lower photoionization energies between 10.0 and 10.9 eV; here, no ion signal should exist since the adiabatic ionization energy was determined to be 10.885 eV.

Nitrogen dioxide ( $\text{NO}_2$ ) and nitrous oxide ( $\text{N}_2\text{O}$ ) account for the detection of the signals at  $m/z = 46$  and  $44$ , respectively; their assignment is confirmed by the agreement between their  $IE_{\text{ad}}$  values of 9.75 eV and 12.88 eV, respectively, and their determined ionization onsets (9.82 and 12.89 eV, respectively). The PIE curve of nitrous oxide ( $\text{N}_2\text{O}$ ) is in accordance with the literature PIE curve (Figure 3q), whereas our PIE curve at  $m/z = 46$  deviates significantly from the literature PIE curve of nitrogen dioxide ( $\text{NO}_2$ ) (Figure 3p) possibly due to fragmentation of nitrogen trioxide ( $\text{NO}_3$ ) at higher photon energies holding an appearance energy of 11.90 eV for  $\text{NO}_2^+$ .

The onset of ion signal of  $m/z = 36$  and  $38$  at 12.74 eV agrees very well with the isotopologues of hydrogen chloride ( $^{35}\text{HCl}$  and  $^{37}\text{HCl}$ ) revealing adiabatic ionization energies of 12.742 eV. Furthermore, both graphs are comparable to the experimental PIE curve from literature recorded for hydrogen chloride (Figures 3r and 3t). In contrast to this, the onset of ion counts for  $m/z = 35$  and  $37$  ( $^{35}\text{Cl}$  and  $^{37}\text{Cl}$ ) of 11.92 eV is much lower by almost 1.0 eV than the ionization energy of atomic chlorine of 12.97 eV (Figures 3s and 3u). This can be explained by the fragmentation of chlorine molecules ( $^{35}\text{Cl}_2$ ,  $^{35,37}\text{Cl}_2$ ,  $^{37}\text{Cl}_2$ ) when absorbing VUV photons; the corresponding **appearance energy of molecular chlorine** was reported to be  $11.86 \pm 0.04$  eV, which lies close to the onset of ionization counts in our experiments. Moreover, the  $\text{Cl}^+$  cations cannot originate from hydrogen chloride ( $\text{HCl}$ ) as it photofragments only above  $17.34 \pm 0.01$  eV. Further, none of the detected chlorine-bearing species such as perchloric acid ( $\text{HClO}_4$ ) or hypochlorous acid ( $\text{HOCl}$ ) are known to yield chlorine cations upon their fragmentation.

The onset of ion signal at  $m/z = 32$  of 12.02 eV correlates nicely with the adiabatic ionization energy of molecular oxygen of 12.07 eV ( $O_2$ , Figure 3v); the PIE curve shows excellent agreement with the literature data, respectively. Ion counts at  $m/z = 30$  can be associated with nitrogen monoxide (NO, Figure 3w), whereas water accounts for the signal at  $m/z = 18$  ( $H_2O$ , Figure 3x). The onset of ion counts obtained for both products are 9.27 eV and 12.62 eV, respectively, which can be compared to the adiabatic ionization energies of 9.26 eV and 12.61 eV<sup>cite</sup>. However, the discrepancy between the actual PIE curve at  $m/z = 30$  with the literature **PIR** curve at higher photoionization energies may be due to the fragmentation of larger nitrogen-oxygen bearing molecules like nitrogen dioxide ( $NO_2$ ,  $AE_{(NO^+)} = 12.34$  eV) and nitric acid ( $HNO_3$ ,  $AE_{(NO^+)} = 13.07$  eV). Nitrous oxide ( $N_2O$ ) does not fragment yielding nitrogen monoxide cations ( $NO^+$ ) below 15.01 eV, and the fragmentation pattern of nitrogen trioxide ( $NO_3$ ) is unknown. The presence of molecular nitrogen ( $N_2$ ) is evident as it appears at photon energies of 16.0 eV and 17.5 eV at the  $m/z = 28$  (Fig. 2c , 2d).

The signal at  $m/z = 17$  can be assigned to the ammonia molecule ( $NH_3$ ) as evident from a comparison of our PIE curve (Figure 3y) with a literature reference **PIE-graph**. Likewise, the **onset of ionization of 10.09 eV [error bar]\_???** agrees well with its experimental adiabatic ionization energy of 10.07 eV. If hydroxyl radicals (OH) are present and contribute to the observed PIE at  $m/z = 17$ , they must originate from the reactions occurring during the pyrolysis of the ammonium perchlorate rather than the photo fragmentation of water ( $H_2O$ ,  $AE_{(OH^+)} = 18.05$  eV) or nitric acid ( $HNO_3$ ,  $AE_{(OH^+)} = 16.6$  eV).

The species holding an  $m/z$  value of 16 can be assigned to the oxygen atom (O); this is well reflected in its ion counts appearing in the PIE curve (Figure 3z) at 13.62 eV; this value agrees well with the ionization energy of atomic oxygen of 13.62 eV. Although the PIE curve depicts similarities at lower photon energies up to 13.5 eV, additional counts at higher photon energies exist most likely from photofragmentation and ionization of chlorine oxides ( $Cl_xO_y$ ) and/or nitrogen oxides ( $N_xO_y$ ) as mentioned above. Namely, oxygen cations may originate from chlorine monoxide (ClO), hypochlorous acid (HOCl), chlorine trioxide ( $ClO_3$ ), perchloric acid ( $HClO_4$ ), or nitrogen trioxide ( $NO_3$ ) whose fragmentation patterns are yet to be discovered. **However**, water ( $H_2O$ ), nitrogen monoxide (NO), molecular oxygen ( $O_2$ ), nitrous oxide ( $N_2O$ ), and nitrogen dioxide ( $NO_2$ ) cannot contribute to the PIE curve since the appearance energy of oxygen cation

( $AE_{(O^+)}$ ) is higher for these compounds than ~~14.5 eV explain what is 14.5eV~~ (19.0 ± 0.2, 20.12, 18.734, 15.31, and 16.82 eV, respectively). Furthermore, neither chlorine dioxide ( $\text{ClO}_2$ ) nor nitric acid ( $\text{HNO}_3$ ) was found to fragment yielding oxygen cations ( $\text{O}^+$ ).

#### 4.2. Possible reaction pathways

The present study revealed the formation of multiple decomposition products of ammonium perchlorate – recorded for the first time on line and *in situ* via photoionization coupled to a reflectron time of flight mass spectrometer. These are compiled in Table 3. These data alone highlight the power of tunable VUV light to ionize and to identify the products based on a comparison of their adiabatic ionization energies and/or their photoionization efficiency curves (PIE) with literature data. In particular, the detection of highly reactive radical transients ( $\text{O}$ ,  $\text{ClO}$ ,  $\text{ClO}_2$ ,  $\text{ClO}_3$ ,  $\text{Cl}$ ,  $\text{NO}_3$ ) underlines the advantage of this approach compared to classical GC-MS and HPLC methods. Here, we are attempting now to propose the actual decomposition pathways.

It has been well-established that the thermal decomposition of ammonium perchlorate ( $\text{NH}_4\text{ClO}_4$ ) starts with a proton transfer from the ammonium cation ( $\text{NH}_4^+$ ) to the perchlorate unit ( $\text{ClO}_4^-$ , ~~R1~~).<sup>2</sup> The products ammonia ( $\text{NH}_3$ ) and perchloric acid ( $\text{HClO}_4$ ) are adsorbed on the surface of the ~~forming~~ cavities inside the crystal then they eventually sublime and take part in various secondary reactions. Both *primary products* are observed in our studies. ~~However~~, these processes that follow the ~~first-initial~~ step are more elusive, and there has been no consensus on the dominating reaction channels ~~in the literature~~.<sup>1</sup> The prominent decomposition pathways might be proposed if the reaction rate constants and the concentration of the species are known. Table S4 (Supplementary Material) lists the rate constants of reactions that may take place in the cavities forming upon the pyrolysis of ammonium perchlorate ( $\text{NH}_4\text{ClO}_4$ ). The equations used to calculate the rate constants were taken from the NIST database accounting for the temperature and the classical activation energies.<sup>50</sup> Although the absolute photoionization cross-sections for multiple products, which is crucial to quantify the concentration of the detected species, are unknown, some conclusions might be drawn by analyzing the rate constants. Most importantly, the decomposition of the primary pyrolysis product perchloric acid ( $\text{HClO}_4$ ) into chlorine trioxide ( $\text{ClO}_3$ ) and hydroxyl ( $\text{OH}$ ) radicals (reaction R2) follows the protonation reaction (R1),

since according to the rate constants, no reactions that could compete with this process exist. It is worth noting that chlorine trioxide ( $\text{ClO}_3$ ) can be detected via the PI-ReTOF-MS setup unambiguously (Section 4.1, Figures 3c and 3d), whereas hydroxyl (OH) radicals are likely to be detected, although its signal at  $m/z = 17$  is masked by the primary decomposition product ammonia ( $\text{NH}_3$ , Figure 3y). Being the only expected decomposition products of perchloric acid ( $\text{HClO}_4$ ), it can be safely assumed that their concentration in the cavities are relatively high making them the most important higher order reactants available during the low-temperature thermal decomposition of ammonium perchlorate ( $\text{NH}_4\text{ClO}_4$ , reaction R3). Therefore they must lead to the formation of chlorine oxides such as chlorine oxide (ClO), atomic and molecular chlorine (Cl and  $\text{Cl}_2$ ), and oxygen (O and  $\text{O}_2$ ), respectively (Supplementary Material). Alternatively, the gradual thermal decomposition of chlorine oxides can also yield the highly reactive oxygen atoms besides chlorine oxides with chlorine in lower oxidation states. These oxidants can then react with ammonia ( $\text{NH}_3$ ) oxidizing it into various nitrogen oxides like nitrogen monoxide (NO) nitrogen dioxide ( $\text{NO}_2$ ), nitric acid ( $\text{HNO}_3$ ), and molecular nitrogen ( $\text{N}_2$ ).

## 5. CONCLUSION

In this *Letter*, the thermal decomposition of the important solid rocket propellant ammonium perchlorate ( $\text{NH}_4\text{ClO}_4$ ) was studied via the PI-ReTOF-MS technique at 483 K at photoionization energies between 9.00 and 17.50 eV. Multiple decomposition products could be identified. These may be classified into three different groups as shown in Table 3: (I) chlorine (II) nitrogen, and (III) oxygen containing compounds, with the first two separated into subgroups. (Ia) denotes the chlorine oxoacids like perchloric acid ( $\text{HClO}_4$ ) and hypochlorous acid (HOCl), (Ib) consist of chlorine oxides such as chlorine trioxide ( $\text{ClO}_3$ ), chlorine dioxide ( $\text{ClO}_2$ ), chlorine monoxide (ClO), whereas class (Ic) contains molecular chlorine ( $\text{Cl}_2$ ), atomic chlorine (Cl), and hydrogen chloride (HCl), respectively. The nitrogen oxoacid nitrous acid ( $\text{HNO}_3$ ) is the only member of subgroup (IIa), class (IIb) consist of nitrogen oxides such as nitrogen trioxide ( $\text{NO}_3$ ), nitrogen dioxide ( $\text{NO}_2$ ), nitrous oxide ( $\text{N}_2\text{O}$ ), and nitrogen monoxide (NO), whereas other nitrogen compounds make up (IIc) like molecular nitrogen ( $\text{N}_2$ ) and ammonia ( $\text{NH}_3$ ). Oxygen compounds are the member of class (III), these are molecular ( $\text{O}_2$ ), atomic oxygen (O), and water ( $\text{H}_2\text{O}$ ).

The PIE curves of the detected species have also been determined in the photoionization energy range of 9.00–14.50 eV; a comparison of these curves and the ionization thresholds to

literature data yielded excellent agreement therefore confirming the assignments. However, further experiments are necessary to obtain absolute photoionization cross-sections of critical reaction products, which would enable the calculation of the concentrations and hence in combination with **rate constants reaction mechanisms**.

## ACKNOWLEDGEMENTS

This work was supported by the Office of Naval Research under Grant N00014-16-1-2078. MA, UA, BX, and the experiments at the chemical dynamics beamline at the ALS are supported by the Director, Office of Science, Office of Basic Energy Sciences, of the U.S. Department of Energy under Contract No. DE-AC02-05CH11231, through the Gas Phase Chemical Physics Program, Chemical Sciences Division.

## References

1. Boldyrev, V. V. Thermal Decomposition of Ammonium Perchlorate. *Thermochim. Acta* 2006, 443, 1–36.
2. Inami, S. H.; Rosser, W. A.; Wise, H. Dissociation Pressure of Ammonium Perchlorate. *J. Phys. Chem.*, 1963, 67, 1077–1079.
3. Jacobs, P. W. M.; Whitehead, H. M. Decomposition and Combustion of Ammonium Perchlorate. *Chem. Rev.* 1969, 69, 551–590.
4. Jacobs, P. W. M.; Pearson, G. S. Mechanism of the Decomposition of Ammonium Perchlorate. *Combust. Flame* 1969, 13, 419–430.
5. Keenan, A. G.; Siegmund, R. F. Thermal Decomposition of Ammonium Perchlorate. *Q. Rev., Chem. Soc.* 1969, 23, 430–452.
6. Singh, G.; Kapoor, I. P. S.; Mannan, S. M., Kaur, Jaspreet. Studies on Energetic Compounds. Part 8: Thermolysis of Salts of  $\text{HNO}_3$  and  $\text{HClO}_4$ . *J. Hazard. Mater.*, 2000, A79, 1–18.
7. Bircumshaw, L. L.; Newman, B. H. The Thermal Decomposition of Ammonium Perchlorate. I. Introduction, Experimental, Analysis of Gaseous Products, And Thermal Decomposition Experiments. *Proc. R. Soc. London, Ser. A* 1954, 227, 115–132.
8. Heath, G. A.; Majer, J. R. Mass Spectrometric Study of the Thermal Decomposition of Ammonium Perchlorate. *Trans. Faraday Soc.* 1964, 60, 1783–1791.
9. Maycock, J. N.; Pai Verneker, V. R.; Jacobs, P. W. M. Mass Spectrometric Study of the Thermal Decomposition of Ammonium perchlorate. *J. Chem. Phys.*, 1967, 46, 2857–2858.
10. Rosser, W. A.; Inami, S. H.; Wise, H. Thermal Decomposition of Ammonium Perchlorate. *Combust. Flame*, 1968, 12, 427–435.
11. Boggs, T. L.; Kraeutle, K. J. Role of the Scanning Electron Microscope in the Study of Solid Rocket Propellant Combustion, I. Ammonium Perchlorate Decomposition and Deflagration. *Combust. Sci. Technol.* 1969, 1, 75–93.
12. Kraeutle, K. J. The Thermal Decomposition of Orthorhombic Ammonium Perchlorate Single Crystals. *J. Phys. Chem.*, 1970, 74, 1350–1356.
13. Dauerman, L.; Kimmel, H.; Wu, Y. J. Application of Internal Reflectance Spectroscopy to the Study of Solid Propellant II: Thermal Decomposition of Ammonium Perchlorate.
14. Boldyrev, V. V.; et al. On the Mechanism of the Thermal Decomposition of Ammonium Perchlorate. *Combust. Flame*, 1970, 15, 71–78.
15. Hackman, E. E.; Hesser, H. H.; Beachell, H. C. Detection of Species Resulting from Condensed Phase Decomposition of Ammonium Perchlorate. *J. Phys. Chem.*, 1972, 76, 3545–3554.
16. Brill, T. B.; Goetz, F. Laser Raman Study of the Thermal Decomposition of Solid  $\text{NH}_4\text{ClO}_4$ . *J. Chem. Phys.*, 1976, 65, 1217–1219.
17. Galwey, A. K.; Mohamed, M. A. The Low Temperature Thermal Decomposition of Ammonium Perchlorate: Nitryl Perchlorate as the Reaction Intermediate.
18. Oxley, J. C.; Smith, J. L.; Valenzuela, B. R. Ammonium Perchlorate Decomposition: Neat and Solution. *J. Energ. Mater.*, 1995, 13, 57–91.
19. Majda, D.; et al. Low-Temperature Thermal Decomposition of Large Single Crystals of Ammonium Perchlorate. *Chem. Phys. Lett.*, 2008, 454, 233–236.
20. Majda, D.; et al. Low-Temperature Thermal Decomposition of Crystalline Partly and Completely Deuterated Ammonium Perchlorate. *Chem. Phys. Lett.*, 2011, 504, 185–188.

21. Zhu, Y.-L.; Huang, H.; Ren, H.; Jiao, Q.-J. Kinetics of Thermal Decomposition of Ammonium Perchlorate by TG/DSC-MS-FTIR. *J. Energ. Mater.*, 32, 16–26.
22. Mallick, L.; Kumar, S.; Chowdhury, A. Thermal Decomposition of Ammonium Perchlorate—A TGA–FTIR–MS Study: Part I. *Thermochim. Acta*, 2015, 610, 57–68.
23. Mallick, L.; Kumar, S.; Chowdhury, A. Thermal Decomposition of Ammonium Perchlorate—A TGA–FTIR–MS Study: Part II. *Thermochim. Acta*, 2017, 653, 83–96.
24. Góbi, S.; Bergantini, A.; Turner, A. M.; Kaiser, R. I. Electron Radiolysis of Ammonium Perchlorate: A Reflectron Time-of-Flight Mass Spectrometric Study. *J. Phys. Chem. A*, 2017, 121, 3879–3890.
25. Zhu, R. S.; Lin, M. C. Towards Reliable Prediction of Kinetics and Mechanisms for Elementary Processes: Key Combustion Reactions of Ammonium Perchlorate. In *Theoretical and Computational Chemistry*; Politzer, P. A., Murray, J. S., Eds.; Elsevier: New Orleans, 2003, Vol. 13, pp. 373–443.
26. Zhu, R. S.; Lin, M. C. *Ab Initio* Chemical Kinetics for ClO Reactions with HO<sub>x</sub>, ClO<sub>x</sub>, and NO<sub>x</sub> ( $x = 1, 2$ ). A Review. *Comput. Theor. Chem.*, 2011, 965, 328–339.
27. Zhu, R. S.; Lin, M. C. *Ab Initio* Study of Ammonium Perchlorate Combustion Initiation Processes: Unimolecular Decomposition of Perchloric Acid and the Related OH + ClO<sub>3</sub> reaction. *PhysChemComm*, 2001, 25, 1–6.
28. Zhu, R. S.; Lin, M. C. *Ab Initio* Studies of ClO<sub>x</sub> reactions. 2. Unimolecular Decomposition of s-ClO<sub>3</sub> and the Bimolecular O + OClO reaction. *J. Phys. Chem. A*, 2002, 106, 8386–8390.
29. Zhu, R. S.; Lin, M. C. *Ab Initio* Studies of ClO<sub>x</sub> reactions. VIII. Isomerization and Decomposition of ClO<sub>2</sub> radicals and Related Bimolecular Processes. *J. Chem. Phys.*, 2003, 119, 2075–2082.
30. Wang, L.; Mebel, A. M.; Yang, X.; Wang, X. *Ab Initio*/RRKM Study of the O(<sup>1</sup>D) + NH<sub>3</sub> Reaction: Prediction of Product Branching Ratios. *J. Phys. Chem. A*, 2004, 108, 11644–11650.
31. Xu, Z. F.; Lin, M. C. Computational Studies on the Kinetics and Mechanisms for NH<sub>3</sub> Reactions with ClO<sub>x</sub> ( $x = 0–4$ ) Radicals. *J. Phys. Chem. A*, 2007, 111, 584–590.
32. Sumathi R., Peyerimhoff, S. D. A Quantum Statistical Analysis of the Rate Constant for the HO<sub>2</sub> + NH<sub>2</sub> reaction. *Chem. Phys. Lett.*, 1996, 263, 742–748.
33. Zhu, R. S., Lin, M. C. *Ab Initio* Study of the ClO + NH<sub>2</sub> Reaction: Prediction of the Total Rate Constant and Product Branching Ratios. *J. Phys. Chem. A*, 2007, 111, 3977–3983.
34. Politzer, P.; Lane, P. Energetics of Ammonium Perchlorate Decomposition Steps. *J. Mol. Struct.: THEOCHEM* 1998, 454, 229–235.
35. Jones, B. M., Kaiser, R. I. Application of Reflectron Time-of-Flight Mass Spectrometry in the Analysis of Astrophysically Relevant Ices Exposed to Ionization Radiation: Methane (CH<sub>4</sub>) and D<sub>4</sub>-Methane (CD<sub>4</sub>) as a Case Study. *J. Phys. Chem. Lett.*, 2013, 4, 1965–1971.
36. Abplanalp, M. J., Borsuk, A., Jones, B. M., Kaiser, R. I. On the Formation and Isomer Specific Detection of Propenal (C<sub>2</sub>H<sub>3</sub>CHO) and cyclopropanone (c-C<sub>3</sub>H<sub>4</sub>O) in Interstellar Model Ices—A Combined FTIR and Reflectron Time-of-Flight Mass Spectrometric Study. *Astrophys. J.*, 2015, 814, 45.

37. Góbi, S., Bergantini, A., Kaiser, R. I., In Situ Detection of Chlorine Dioxide (ClO<sub>2</sub>) in the Radiolysis of Perchlorates and Implications for the Stability of Organics on Mars. *Astrophys. J.*, 2016, 832, 164.
38. Glavin, D. P., et al. Evidence for Perchlorates and the Origin of Chlorinated Hydrocarbons Detected by SAM at the Rocknest Aeolian Deposit in Gale Crater. *J. Geophys. Res.: Planets*, 2013, 118, 1955–1973.
39. Leshin, L. A., et al. Volatile, Isotope, and Organic Analysis of Martian Fines with the Mars Curiosity Rover. *Science*, 2013, 341, 1238937.
40. Parker, D. S. N.; Kaiser, R. I. On the Formation of Nitrogen-Substituted Polycyclic Aromatic Hydrocarbons (NPAHs) in Circumstellar and Interstellar Environments. *Chem. Soc. Rev.*, 2017, 46, 452.
41. Weitzel, K.-M.; Mahnert, J.; Penno, M. ZEKE-PEPICO Investigations of Dissociation Energies in Ionic Reactions. *Chem. Phys. Lett.*, 1994, 224, 371–380.
42. Moore, C. E. Ionization Potentials and Ionization Limits Derived from the Analyses of Optical Spectra. *Natl. Stand. Ref. Data Ser.*, (U.S. Natl. Bur. Stand.), 1970, 34, 1–30.
43. Li, Y. Y.; Qi, F. Recent Applications of Synchrotron VUV Photoionization Mass Spectrometry: Insight into Combustion Chemistry. *Acc. Chem. Res.*, 2010, 43, 68–78.
44. Qi, F.; Yang, R.; Yang, B.; Huang, C. Q.; Wei, L. X.; Wang, J.; Sheng, L. S.; Zhang, Y. W. Isomeric Identification of Polycyclic Aromatic Hydrocarbons Formed in Combustion With Tunable Vacuum Ultraviolet Photoionization. *Rev. Sci. Instrum.*, 2006, 77, 084101.
45. Qi, F. Combustion Chemistry Probed by Synchrotron VUV Photoionization Mass Spectrometry. *Proc. Combust. Inst.*, 2013, 34, 33–63.
46. Cool, T. A.; Nakajima, K.; Taatjes, C. A.; McIlroy, A.; Westmoreland, P. R.; Law, M. E.; Morel, A. Studies of a Fuel-Rich Propane Flame With Photoionization Mass Spectrometry. *Proc. Combust. Inst.*, 2005, 30, 1681–1688.
47. Cool, T. A.; Wang, J.; Nakajima, K.; Taatjes, C. A.; McIlroy, A. Photoionization Cross Sections for Reaction Intermediates in Hydrocarbon Combustion. *Int. J. Mass spectrom.* 2005, 247, 18–27.
48. Oßwald, P.; Gülденberg, H.; Kohse-Höinghaus, K.; Yang, B.; Yuan, T.; Qi, F. Combustion of Butanol Isomers – A Detailed Molecular Beam Mass Spectrometry Investigation of Their Flame Chemistry. *Combust. Flame*, 2011, 158, 2–15.
49. Photoionization Cross Section Database (Version 1.0). National Synchrotron Radiation Laboratory, Hefei, China. <http://flame.nsrl.ustc.edu.cn/database/>
50. NIST Chemical Kinetics Database Standard Reference Database 17, Version 7.0 (Web Version), Release 1.6.8, Data Version 2017.07. <http://kinetics.nist.gov/kinetics/>

**Table 1.** Previous Experimental Results on the Low-Temperature Decomposition of Ammonium Perchlorate.

$p$ (mbar)	$T$ (K)	Detection	Products	Reference
‘vacuum’	493–553	Chemical analysis	HClO <sub>4</sub> , ClO <sub>2</sub> , Cl <sub>2</sub> , HCl, H <sub>2</sub> O, N <sub>2</sub> , O <sub>2</sub> , N <sub>2</sub> O, N <sub>2</sub> O <sub>4</sub>	7
‘very low pressure conditions’	393–473	MS	Various fragments of NH <sub>4</sub> ClO <sub>4</sub> and HClO <sub>4</sub>	8
10 <sup>-3</sup>	503	MS	H <sub>2</sub> O, N <sub>2</sub> O, Cl <sub>2</sub> , O <sub>2</sub> , HCl, N <sub>2</sub>	9
‘in He flow’	523–598	GC, Chemical Analysis	O <sub>2</sub> , N <sub>2</sub> , N <sub>2</sub> O, Cl <sub>2</sub> , ClO <sub>2</sub> , HNO <sub>3</sub> , HCl, NO	10
27	499	SEM	–	11
1000	484–504	OM	–	12
N/A	523	ATR IR	No products could be identified	13
N/A	523–773	TOF-MS	NH <sub>3</sub> , HClO <sub>4</sub> , ClO <sub>3</sub> , ClO <sub>2</sub> , ClO, Cl, NH <sub>2</sub> HClO <sub>4</sub> , ClO <sub>3</sub> , ClO <sub>2</sub> , ClO, HCl, Cl, O <sub>2</sub> , HNO, NO, NH <sub>4</sub> , NH <sub>3</sub> , OH, NH <sub>2</sub> , NH	14
10 <sup>-5</sup>	368–438	TOF-MS		15
‘in N <sub>2</sub> flow’	300–625	Raman spectroscopy	No products were identified	16
N/A	460–510	Gas analysis, SEM	NO <sub>2</sub> ClO <sub>4</sub> intermediate, NO <sup>+</sup> , ClO <sub>3</sub> <sup>-</sup> , 2O, O <sub>2</sub> , N <sub>2</sub>	17
‘in N <sub>2</sub> flow’	488–658	DSC, HPLC, GC	O <sub>2</sub> , Cl <sup>-</sup> , N <sub>2</sub> O, ClO <sub>3</sub> <sup>-</sup> , N <sub>2</sub> , Cl <sub>2</sub> , NH <sub>4</sub> <sup>+</sup>	18
27	293–623	DSC, TGA, SEM, QMS	N <sub>2</sub> O, NO	19,20
‘in Ar flow’	303–773	TGA/DSC–FT-IR/MS	N <sub>2</sub> O, NO <sub>2</sub>	21
‘low pressures’	303–773	TGA–FT-IR/MS	<b>FT-IR:</b> N <sub>2</sub> O, HCl, NO <sub>2</sub> , HNO <sub>3</sub> <b>QMS:</b> H <sub>2</sub> O, Cl <sub>2</sub> , O <sub>2</sub> <b>FT-IR:</b> NH <sub>3</sub> , N <sub>2</sub> O, HCl, NO <sub>2</sub> , H <sub>2</sub> O, NO, HNO <sub>3</sub>	22
‘low pressures’	303–77103	TGA–FT-IR/MS	<b>QMS:</b> Cl <sub>2</sub> , O <sub>2</sub> , HOCl, ClO, NH <sub>4</sub> Cl	23



**Table 2.** Pyrolysis Products Detected in the Ammonium Perchlorate Sample via the PI-ReTOF-MS Technique. +/- denotes presence or absence at that particular photon energy

<i>m / z</i>	Assignment	<i>IE</i> (eV)		Photon Energy (eV)			
		Adiabatic	Vertical	12.0	14.0	16.0	17.5
16	O	13.618	13.618	–	+	+	+
17	NH <sub>3</sub>	10.069 ± 0.002	10.82 <sup>b</sup>	+	+	–	–
	(OH) <sup>c</sup>	13.0170 ± 0.0002	13.01 <sup>b</sup>				
18	H <sub>2</sub> O	12.6188 ± 0.0009	12.60 ± 0.02 <sup>b</sup>	–	+	+	+
28 <sup>a</sup>	N <sub>2</sub>	15.581 ± 0.008	15.58 <sup>b</sup>	–	–	+	+
30	NO	9.2643 ± 0.0002	9.26 <sup>b</sup>	+	+	–	+
32	O <sub>2</sub>	12.0697 ± 0.0002	12.33 ± 0.01 <sup>b</sup>	+	+	+	+
35	<sup>35</sup> Cl	12.97 ± 0.02 <sup>b</sup>	12.97 ± 0.02 <sup>b</sup>	–	+	+	+
36	H <sup>35</sup> Cl	12.742 ± 0.010	12.742 ± 0.010	–	+	+	+
37	<sup>37</sup> Cl	12.97 ± 0.02 <sup>b</sup>	12.97 ± 0.02 <sup>b</sup>	–	+	+	+
38	H <sup>37</sup> Cl	12.742 ± 0.010	12.742 ± 0.010	–	+	–	–
44	N <sub>2</sub> O	12.88 ± 0.005	12.89 <sup>b</sup>	–	+	+	+
46	NO <sub>2</sub>	9.75 ± 0.01	11.23 <sup>b</sup>	+	+	+	+
51	<sup>35</sup> ClO	10.885 ± 0.016	11.01 ± 0.01 <sup>b</sup>	+	+	–	–
	(NH <sub>2</sub> Cl) <sup>c</sup>	9.85 ± 0.02 <sup>b</sup>	10.52 ± 0.01 <sup>b</sup>				
52	HO <sup>35</sup> Cl	11.12 ± 0.01 <sup>b</sup>	11.22 ± 0.01 <sup>b</sup>	+	+	–	–
53	<sup>37</sup> ClO	10.885 ± 0.016	11.01 ± 0.01 <sup>b</sup>	+	+	–	–
	(NH <sub>2</sub> Cl) <sup>c</sup>	9.85 ± 0.02 <sup>b</sup>	10.52 ± 0.01 <sup>b</sup>				
54	HO <sup>37</sup> Cl	11.12 ± 0.01 <sup>b</sup>	11.22 ± 0.01 <sup>b</sup>	+	+	–	–
62	NO <sub>3</sub>	12.57 ± 0.03	12.57 ± 0.03				
	(NH <sub>2</sub> NO <sub>2</sub> ) <sup>c</sup>	11.02 ± 0.06 <sup>b</sup>	11.75 <sup>b</sup>	+	+	–	–
	(HON=NOH) <sup>c</sup>	N/A	N/A				
63	HNO <sub>3</sub>	11.95 ± 0.01	12.2 <sup>b</sup>	+	+	–	–
67	<sup>35</sup> ClO <sub>2</sub>	10.33 ± 0.02 <sup>b</sup>	10.475 ± 0.005 <sup>b</sup>	+	+	–	–
69	<sup>37</sup> ClO <sub>2</sub>	10.33 ± 0.02 <sup>b</sup>	10.475 ± 0.005 <sup>b</sup>	+	+	–	–

70	$^{35}\text{Cl}_2$			+	+	+	+
72	$^{35}\text{Cl}^{37}\text{Cl}$	$11.48 \pm 0.01$	11.49	+	+	+	+
74	$^{37}\text{Cl}_2$			+	+	+	+
83	$^{35}\text{ClO}_3$	$11.4 \pm 0.1^{\text{d}}$	N/A	-	+	-	-
85	$^{37}\text{ClO}_3$			-	+	-	-
100	$\text{H}^{35}\text{ClO}_4$	$12.37^{\text{b}}$	$12.37^{\text{b}}$	-	+	+	+
102	$\text{H}^{37}\text{ClO}_4$			-	+	-	-

For the reference list see Table S2 in the Supplementary Material.

<sup>a</sup> Ionization energy higher than 14.5 eV, therefore N<sub>2</sub> is not included in Figure 3.

<sup>b</sup> Values obtained by Photoelectron Spectroscopy.

<sup>c</sup> Alternative, tentative assignment.

<sup>d</sup> Values obtained by Electron Ionization technique.

**Table 3.** Species observed by the present study classified based on their oxidation states and molecule classes. The species in parentheses are tentative assignments.

Ox. state	Class						
	Cl-compounds			N-compounds		O-compounds	
	Ia	Ib	Ic	IIa	IIb	IIc	III
+7	HClO <sub>4</sub>						
+6		ClO <sub>3</sub>			NO <sub>3</sub>		
+5				HNO <sub>3</sub>			
+4		ClO <sub>2</sub>			NO <sub>2</sub>		
+3							
+2		ClO			NO		
+1	HClO				N <sub>2</sub> O		
0			Cl, Cl <sub>2</sub>			N <sub>2</sub>	O, O <sub>2</sub>
-1			HCl				
-2							H <sub>2</sub> O
-3						NH <sub>3</sub>	

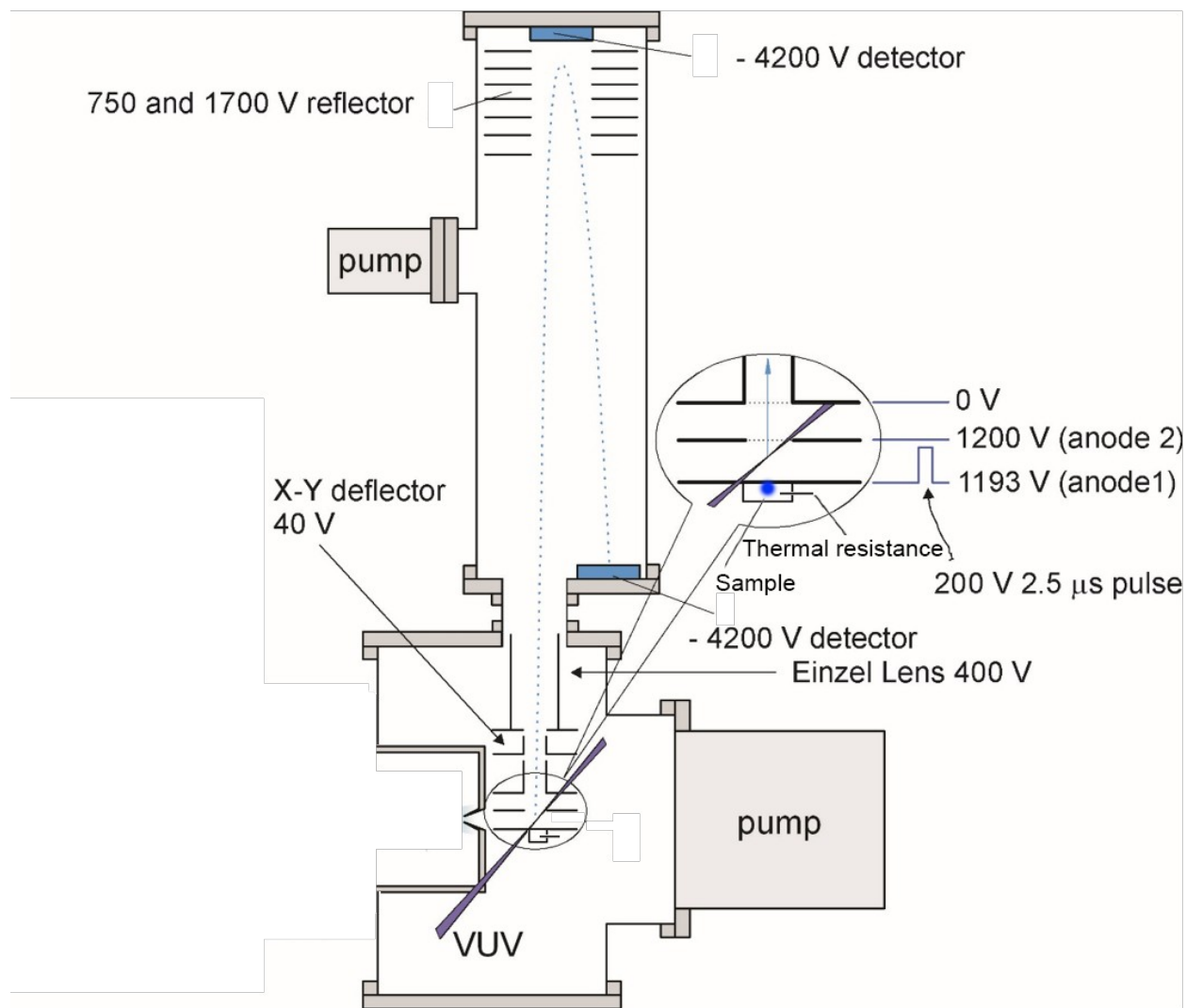


**Figure 1** Schematic view of the experimental setup.

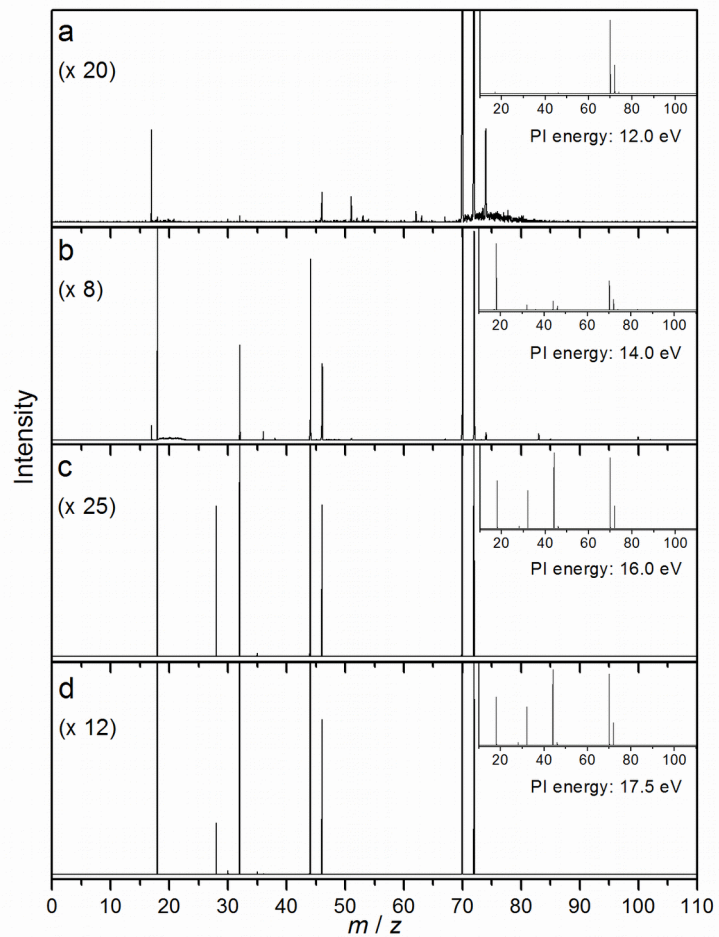


**Figure 2** PI-ReTOF-MS spectra of the degradation products of ammonium perchlorate recorded at photoionization energies of 12.0 eV (**a**), 14.0 eV (**b**), 16.0 eV (**c**), and 17.5 eV (**d**) up to  $m/z = 110$ . The insets show the full spectra without magnification.

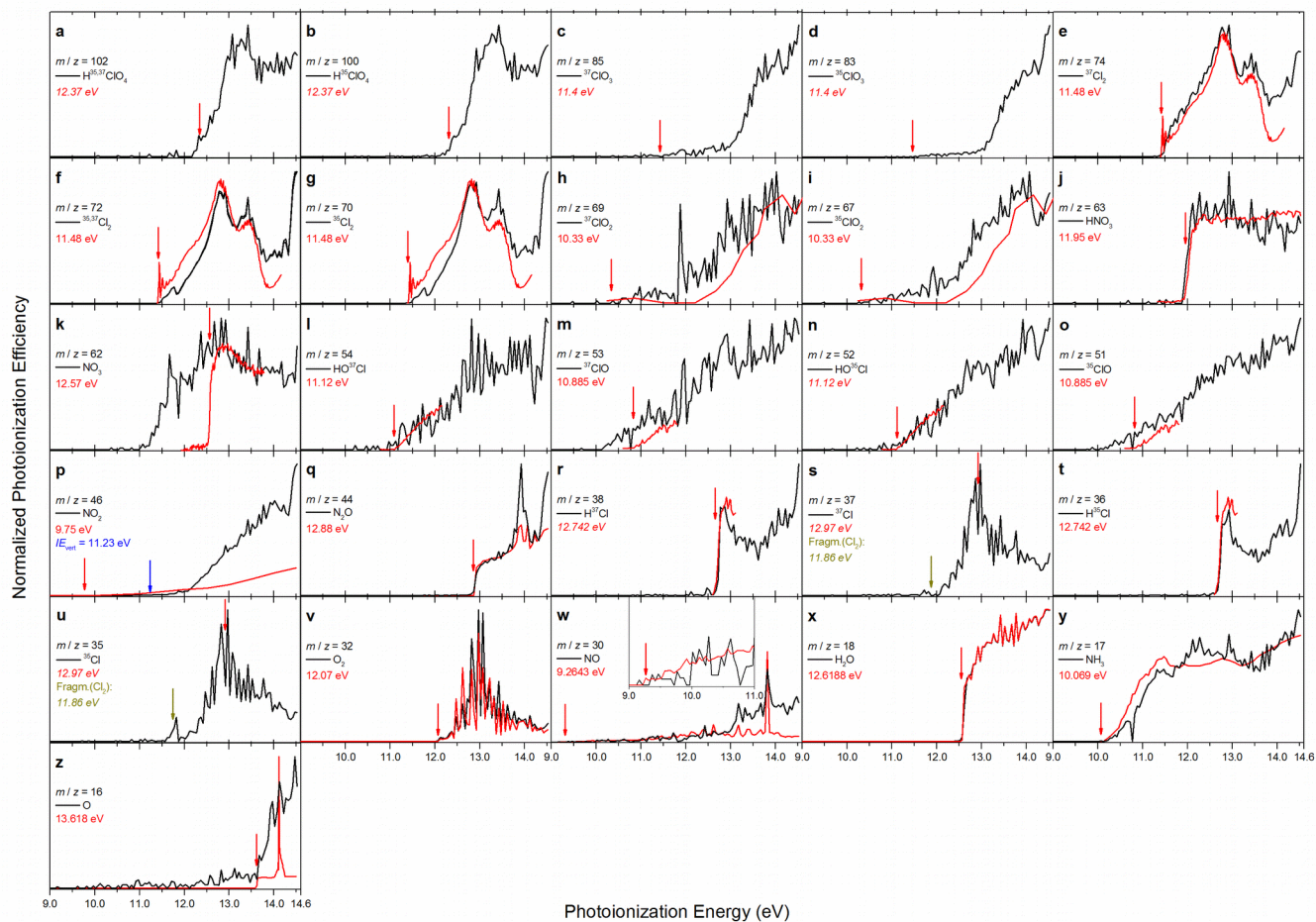


**Figure 3** Photoionization efficiency curves of the pyrolysis products of ammonium perchlorate; experimental data taken from previous works are plotted as solid red lines (where available). The adiabatic ionization energies ( $IE_{ad}$ ) are marked with a red arrow, vertical ionization energies ( $IE_{vert}$ ) with a blue arrow, whereas appearance energies ( $AE$ ) of fragments are marked with a yellow arrow.